



## Synthesis and properties of $\text{La}_{0.6}\text{Sr}_{0.4}\text{CoO}_{3-\delta}$ nanopowder

Youkun Tao, Jing Shao, Jianxin Wang, Wei Guo Wang\*

Division of Fuel cell and Energy Technology, Ningbo Institute of Material Technology & Engineering, Chinese Academy of Sciences, Ningbo 315201, People's Republic of China

### ARTICLE INFO

#### Article history:

Received 1 August 2008

Received in revised form 9 September 2008

Accepted 9 September 2008

Available online 18 September 2008

#### Keywords:

$\text{La}_{0.6}\text{Sr}_{0.4}\text{CoO}_{3-\delta}$

Nanopowder

Cathode

Polarization resistance

### ABSTRACT

Uniform nanopowders of  $\text{La}_{0.6}\text{Sr}_{0.4}\text{CoO}_{3-\delta}$  (LSC) were synthesized by the combined citrate–EDTA method. The precursor solution was prepared from nitrates of the constituent metal ion, citric acid and EDTA with a pH value controlled by ammonia. The obtained product was characterized by TG/DTA, XRD, SEM, and BET measurements. The single perovskite phase could form completely after sintering at the temperature of 900 °C. There was no significant effect of the precursor solution pH value on the perovskite phase formation temperature; however, LSC powders prepared from the precursors with different pH values showed specific shapes. The morphology of  $\text{La}_{0.6}\text{Sr}_{0.4}\text{CoO}_{3-\delta}$  powder was also optimized with proper surfactant addition. The sintered  $\text{La}_{0.6}\text{Sr}_{0.4}\text{CoO}_{3-\delta}$  bulk samples exhibited an electrical conductivity of 1867  $\text{S cm}^{-1}$  in air at 800 °C. The impedance spectra of a symmetric LSC cathode on a GDC electrolyte substrate were measured and polarization resistance ( $R_p$ ) values of 0.17  $\Omega \text{ cm}^2$  at 700 °C and 0.07  $\Omega \text{ cm}^2$  at 750 °C in air were obtained.

© 2008 Elsevier B.V. All rights reserved.

### 1. Introduction

Solid oxide fuel cells (SOFCs) are considered as one of the most promising future power generation devices. In addition to the high energy conversion efficiency, SOFCs have other advantages such as an all solid configuration, multi-fuel capability, a modular construction design and environmental compatibility. A conventional SOFC using  $\text{La}_{1-x}\text{Sr}_x\text{MnO}_{3-\delta}$  (LSM) as the cathode has to work at high temperatures of 800–1000 °C [1–3], which leads to many disadvantages in the selection of interconnects and sealing materials. Intermediate temperature–solid oxide fuel cells (IT-SOFCs) can operate between 600 °C and 800 °C, temperatures at which inexpensive ferritic stainless steel (Fe–Cr alloy) could be used for the interconnectors [4,5], while the chemical and mechanical durability of all the components would be enhanced [6–8]. At low operating temperatures, however, the ion conductivity of the YSZ electrolytes and the performance of the LSM cathode decrease rapidly. Hence, besides reducing ohmic losses in electrolytes [9–12], it is essential to develop cathode materials with better catalytic ability to substitute LSM. A candidate cathode should be fabricated using materials of excellent catalytic ability and a large three-phase boundary (TPB) as the electrochemical reaction site. Mixed ionic–electronic conductors (MIECs) like doped lanthanum cobaltites provide a higher reaction rate of oxygen reduction with enlarged reaction sites and have been extensively studied as cathode materials for SOFCs [1,2,13].

A number of approaches such as solid-state reactions, mechanical-synthesis [14], co-precipitation [15,16], solution combustion or thermal decomposition [17–19], hydro-thermal and the Pechini method [20,21], have been used to synthesize  $\text{LaCoO}_3$ -based perovskite powders. The Pechini method was highly attractive because various metal ions are chelated to form metal complexes in solution and are uniformly distributed at the molecular level. Citric acid, urea and EDTA are usually utilized as complexing agents, among which, EDTA is a good chelating agent for transition metal cations, and the combined citrate–EDTA method [22–24] is particularly useful for synthesizing ultra-fine powders of complex oxide compositions. A wide variety of powders such as  $\text{La}_{0.6}\text{Sr}_{0.4}\text{Co}_{0.2}\text{Fe}_{0.8}\text{O}_{3-x}$  [23],  $\text{Ba}_{0.5}\text{Sr}_{0.5}\text{Co}_{0.8}\text{Fe}_{0.2}\text{O}_{3-x}$  [22,24],  $\text{La}_{0.6}\text{Ba}_{0.4}\text{Co}_{0.2}\text{Fe}_{0.8}\text{O}_{3-x}$  [24], and  $\text{La}_{0.9}\text{Sr}_{0.1}\text{Ga}_{0.8}\text{Mg}_{0.2}\text{O}_{2.85}$  [25] have been synthesized recently by this approach.

With respect to the cathodes and catalytic reactions, it is desirable to synthesize ultra-fine powders of doped lanthanum cobaltites with good crystallization, uniform shape and narrow size distribution. Although  $\text{La}_{0.6}\text{Sr}_{0.4}\text{CoO}_{3-\delta}$  (LSC) particles with nanoscaled grain size were synthesized in some reports, powders with uniform size and low agglomeration were difficult to obtain. The pure perovskite structure of LSC formed at a temperature exceeding 1000 °C is in a condition which caused the nanopowders to sinter together into large agglomerates. Hence, it is of great interest to synthesize LSC nanopowders with a pure cubic perovskite structure and uniform size at lower temperatures.

The traditional citrate–EDTA complexing procedure was carried out in alkaline solution. In the present study, the modification of this procedure was performed by adjusting the pH values of the precursor solution in the acid range; particularly, appropriate sur-

\* Corresponding author. Tel.: +86 574 8791 1363; fax: +86 574 8668 5139.  
E-mail address: [wgwang@nimte.ac.cn](mailto:wgwang@nimte.ac.cn) (W.G. Wang).

factant additions were used to optimize the shape of the powders. The influence of the pH condition on the phase forming and morphology of the resultant LSC powder was investigated; the amount of the surfactant additions was also studied. The electrical conductivities of the sintered bulk sample of LSC were measured at various temperatures. The symmetrical cell of the LSC cathode was prepared on the GDC substrate and the electrical performance study was carried out.

## 2. Experimental procedure

### 2.1. Powder synthesis

The starting materials used in the synthesis:  $\text{La}_2\text{O}_3$  (99.99% purity),  $\text{Sr}(\text{NO}_3)_2$  (99.99% purity),  $\text{Co}(\text{NO}_3)_2 \cdot 6\text{H}_2\text{O}$  (99.99% purity), and citric acid (CA) (99% purity), EDTA (99% purity), were all obtained from Sinopharm Chemical Reagent Co., Ltd. The synthesis of the powders by the citrate–EDTA method is shown as a flow chart in Fig. 1. To yield 11 g of the final  $\text{La}_{0.6}\text{Sr}_{0.4}\text{CoO}_{3-\delta}$  (LSC) powder, a stoichiometric amount of  $\text{La}_2\text{O}_3$  was dissolved in nitric acid and other constituent metal nitrates were subsequently added. The solution was heated in a water bath at the temperature of  $75^\circ\text{C}$ . Calculated amounts of citric acid (CA) and EDTA with ratios to overall metal ion content of 1.5:0.5:1 was added to the metal nitrate aqueous solution in sequence. The initially clear solution obtained a transparent red coloration after adding CA, and turned dark violet some 10 min later after dissolving EDTA in the solution. The pH value of the solution was measured to be 0.5; the pH value was adjusted to 2.5, 5.4 and 8.0 by adding ammonia in order to study its effect on the synthesis process. Lastly, a definite amount polyethylene glycol (PEG) was added as a surfactant, and the resultant solutions were denoted as S1 ( $9 \times 10^{-3} \text{ g ml}^{-1}$ ), S2 ( $8 \times 10^{-3} \text{ g ml}^{-1}$ ), S3 ( $1 \times 10^{-2} \text{ g ml}^{-1}$ ), S4 ( $2 \times 10^{-2} \text{ g ml}^{-1}$ ) and S5 ( $4 \times 10^{-2} \text{ g ml}^{-1}$ ). The precursor solution was heated and stirred continuously for several hours to evaporate the water and to undergo polyesterification. The resulting viscous dope was dried at  $110^\circ\text{C}$  for 12 h until it became slightly swollen and then dried at  $250^\circ\text{C}$  for 5 h. At last, the black ash was heat treated at  $900^\circ\text{C}$  for 3 h.

### 2.2. Powder characterization

To study the pyrolysis behavior and the phase evolution of the gel precursor dried at  $110^\circ\text{C}$ , TG/DTA analysis was carried out with a

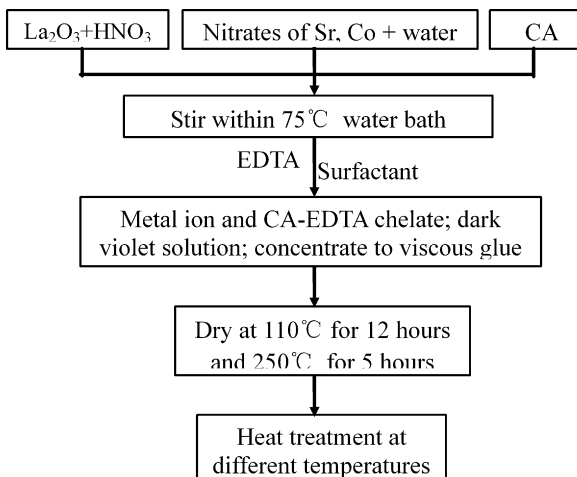


Fig. 1. Flow chart of LSC synthesis by the citrate–EDTA method.

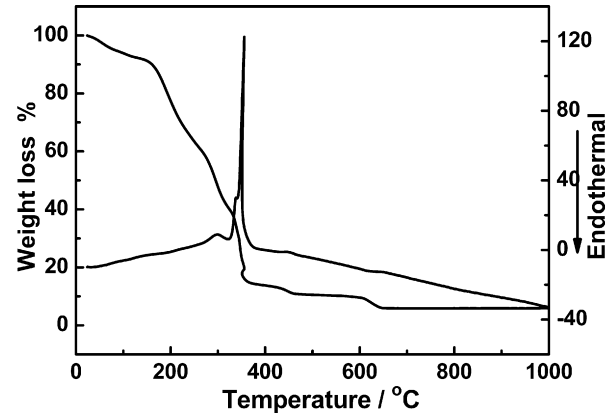


Fig. 2. TG/DTA curves of the as-synthesized LSC precursors.

heating velocity of  $5^\circ\text{C min}^{-1}$  under air. After calcining in stagnant air, the phase evolution of the resulting powder was investigated by X-ray diffraction (XRD). XRD data were collected using a Bruker D8 Advance with  $\text{CuK}\alpha$  radiation at a step of  $0.02^\circ \text{ s}^{-1}$  in the range of  $2\theta$  from  $20^\circ$  to  $80^\circ$ . After grinding for a few minutes with a mortar, the morphologies of the synthesized powders were characterized by means of scanning electron microscopy (SEM) using a Hitachi S-4800 microscope. BET specific surface areas were measured by the nitrogen adsorption–desorption at liquid nitrogen temperature.

The resultant LSC powders were pressed into bars of  $25 \times 8 \times 3 \text{ mm}$  under 300 MPa pressure, and then sintered at  $1200^\circ\text{C}$  or  $1250^\circ\text{C}$  for 5 h, respectively. The electrical conductivity of the bulk samples at different temperatures was measured by the four-probe DC measurement method.

### 2.3. Symmetric cell fabrication and measurement

$\text{Ce}_{0.9}\text{Gd}_{0.1}\text{O}_{1.95}$  (GDC) electrolytes of 0.2 mm thickness were prepared by tape casting and sintered at  $1450^\circ\text{C}$ . A cathode slurry of 10 g LSC perovskite powders (prepared with optimized condition), 1 g PVP and 20 ml ethanol was mixed and ball-milled for 24 h. The slurry was sprayed onto both sides of the CGO electrolyte to fabricate a symmetric cell and sintered at  $950^\circ\text{C}$  for 2 h. The cell was cut to dimensions of 7 mm by 7 mm and painted with platinum paste. The area-specific resistance of the cathode was measured using the four-terminal AC impedance method with a Soltron 1260 analyzer over the frequency range from 2 MHz to 0.1 Hz using 20 mV excitation voltage at  $600\text{--}800^\circ\text{C}$  in air. The microstructure of the symmetric cell was also examined by SEM using a Hitachi S-4800 microscope.

## 3. Results and discussion

### 3.1. TG/DTA

Fig. 2 shows the TG/DTA curves of the LSC precursors obtained at a heating rate of  $5^\circ\text{C min}^{-1}$  in air from room temperature to  $1000^\circ\text{C}$ . The as-synthesized precursor was derived from a solution comprising Surfactant1 and a pH value of 0.5. The first weight loss occurred during the heating step from room temperature to  $160^\circ\text{C}$ , resulting from the dehydration and decomposition of nitrates. From  $160^\circ\text{C}$  to about  $360^\circ\text{C}$ , a weight loss of about 75% was observed, which corresponded to the decarbonization of the residual organic compound. The DTA curve revealed a strong and sharp exothermic peak with a vertex at  $356^\circ\text{C}$ , which was likely due to the oxidation or combustion of the chelate complex along

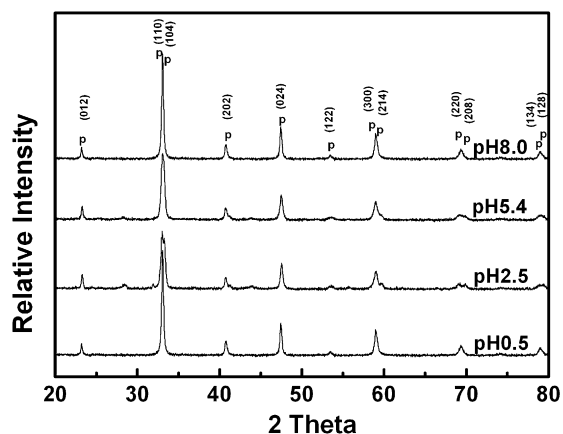


**Fig. 3.** XRD patterns of LSC powders after 900 °C heat treatment. The powders were synthesized from precursor solutions of different pH value. “p”– perovskite LSC.

with the forming of metal oxides. Between 600 °C and 650 °C, the TG curve showed a weight loss of about 5%, while the DTA curve showed an endothermic peak at 628 °C. These peaks may be ascribed to the decomposition or solid state reaction of the carbonate intermediates. From 700 °C to 1000 °C, the DTA curve showed no further endo- or exo-thermal peak, and very little weight loss was observed.

### 3.2. Effect of pH value

#### 3.2.1. XRD

XRD patterns for the heat treated LSC powders are shown in Fig. 3. All samples were heat treated at 900 °C for 3 h after previ-

**Table 1**

Specific surface area of LSC powders derived from precursors of different pH conditions.

Sample	pH value of solution	Specific surface ( $\text{m}^2 \text{g}^{-1}$ )
PH0.5	0.5	7.14
PH2.5	2.5	7.55
PH5.4	5.4	4.79
PH8.0	8.0	5.40

ously dwelling at 800 °C for 2 h. In this study, we referred to the LSC powders prepared from the solutions with pH values of 0.5, 2.5, 5.4 and 8.0, as PH0.5, PH2.5, PH5.4, PH8.0, respectively, and the surfactant additions were all fixed at S1. The single perovskite phase was formed for samples PH8.0 and PH0.5 after heat treatment at 900 °C for 3 h; while for PH5.4 and PH2.5, both resultant powders were observed to have a tiny impure phase with a characteristic peak at  $\theta = 28.39^\circ$ . PH2.5 has an additional peak at  $\theta = 31.87^\circ$ , as shown in Fig. 3. In this regard, a precursor solution with a pH value of 8.0 or 0.5 seems to favor the chelation between metal ions and CA–EDTA and facilitates the crystallization. As a whole, the pH value of the solution has an effect on the chelating process but inconspicuously. All the samples calcined at 1000 °C were fully developed into the single perovskite structure.

#### 3.2.2. BET analysis

After heat treatment of the as-synthesized LSC powders at 900 °C for 3 h, the specific surface area was measured by BET measurements and the results given in Table 1. Samples PH0.5 and PH2.5 have specific surface areas of  $7.14 \text{ m}^2 \text{g}^{-1}$  and  $7.55 \text{ m}^2 \text{g}^{-1}$ , respectively; both specific surface areas are larger than that of samples PH5.4 and PH8.0.

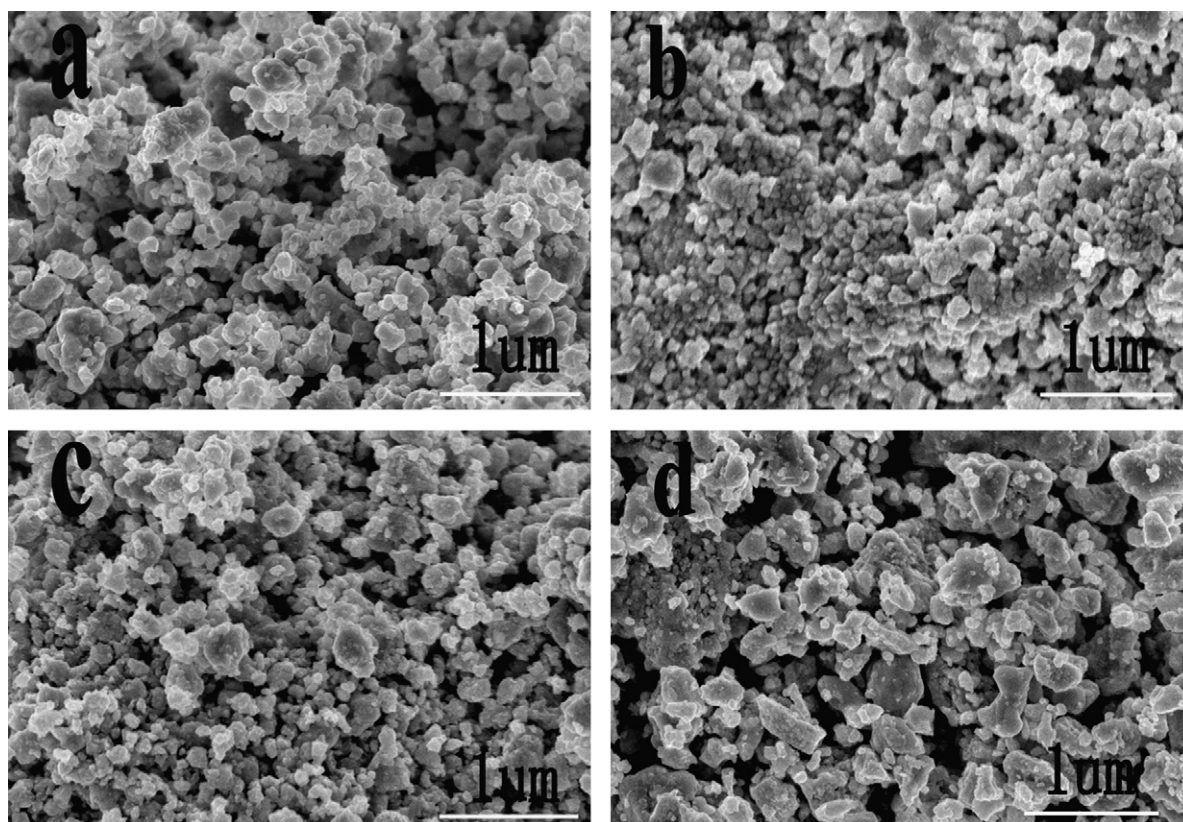


**Fig. 4.** SEM micrographs of LSC powders synthesized from solutions of different pH condition: (a) PH0.5 (b) PH2.5 (c) PH5.4 (d) PH8.0.

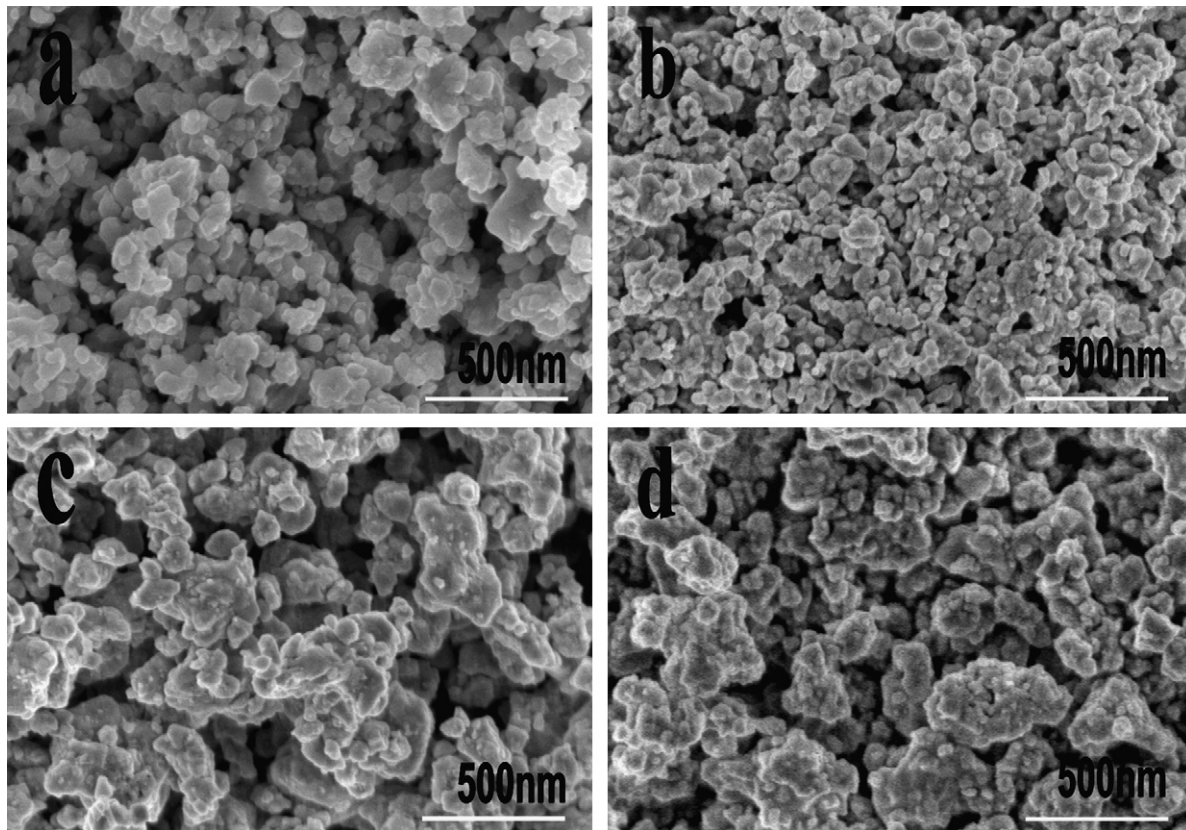


Fig. 5. SEM micrographs of LSC powders synthesized with different surfactant additions: (a) S2 (b) S3 (c) S4 (d) S5.

### 3.2.3. SEM

The morphologies of the LSC powders derived from the different pH-valued precursors are presented in Fig. 4. The samples were all synthesized with surfactant1 and heat treated at 900 °C for 3 h. For LSC originated from low pH valued precursors (pH 0.5, 2.5 and 5.4), the size of the powder particles were small and uniform; when the pH value was adjusted to 8.0 with ammonia, increased and serious aggregation was observed, as is shown in Fig. 4. Sample PH2.5 had the smallest particle size but was aggregated, while the best powder morphology was found in sample PH0.5 in which case the particles were uniform and well dispersed. This study indicated that the morphology of the LSC powder could be tailored by controlling the pH values in the synthesis process.

### 3.3. Effect of surfactant

In our previous study, it was found that the addition of surfactant to the solution had an important effect on the shape optimization of the LSC powders: the powders synthesized without surfactant addition sintered together to form micron-scaled agglomerates after calcining at 900 °C; when a small amount of surfactant (S1) was added, a uniform and dispersed powder was achieved in sample PH0.5, as shown in Fig. 4(a). Accordingly, various surfactant additions were investigated; based on the pH effect studied above, the pH values of the precursor solutions were all fixed at 0.5. Fig. 5(a) shows the SEM micrographs of  $\text{La}_{0.6}\text{Sr}_{0.4}\text{CoO}_{3-\delta}$  powders synthesized from precursor solutions with S2. The powder calcined at 900 °C for 3 h was found to have nanoscaled size particles of about 60 nm and the specific surface area was measured to be  $8.22\text{ m}^2\text{ g}^{-1}$ . Compared with S1 (Fig. 4a), the powder size was much smaller; both surfactant additions resulted in the for-

mation of uniform and dispersed powders with low agglomerates. The powder originated from the precursor with S3 has the smallest size, but slight agglomeration was formed. From S4 to S5, the resultant powders tend to agglomerate more and more seriously, as is observed in Fig. 5. So the optimized shape of the LSC can be achieved when the pH value of the precursor was 0.5 and S2 was added.

The uniform shape and nanosize of the resulting powders originated from the precursor. During the chelation reaction, all the reactants were uniformly mixed in solution at the atomic or molecular level. And as a consequence of proper surfactant addition, the polymeric macromolecules absorbed on the colloidal particles were likely to undergo polymerization with the carboxyl of CA

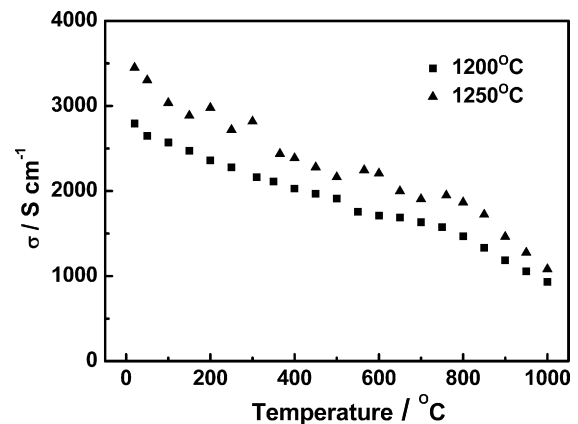


Fig. 6. Electrical conductivity of the LSC bulk sample sintered at 1250 °C and 1200 °C.

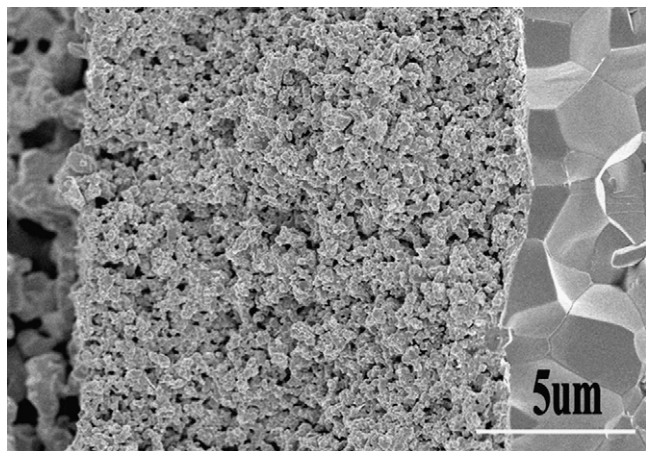


Fig. 7. Cross-section SEM micrograph of the LSC cathode on the GDC electrolyte substrate sintered at 950 °C for 2 h.

or EDTA. The addition of surfactants performed in terms of steric interactions by enlarging the distance between colloids thereby reducing interpenetration [26]. Moreover, a large volume of gases evolved during desiccation limited the degree of inter-particle contact. Consequently, the nucleation process occurred through the rearrangement and short-distance diffusion of nearby atoms and molecules, and the initial nanosize of the powders was retained after heat treatment.

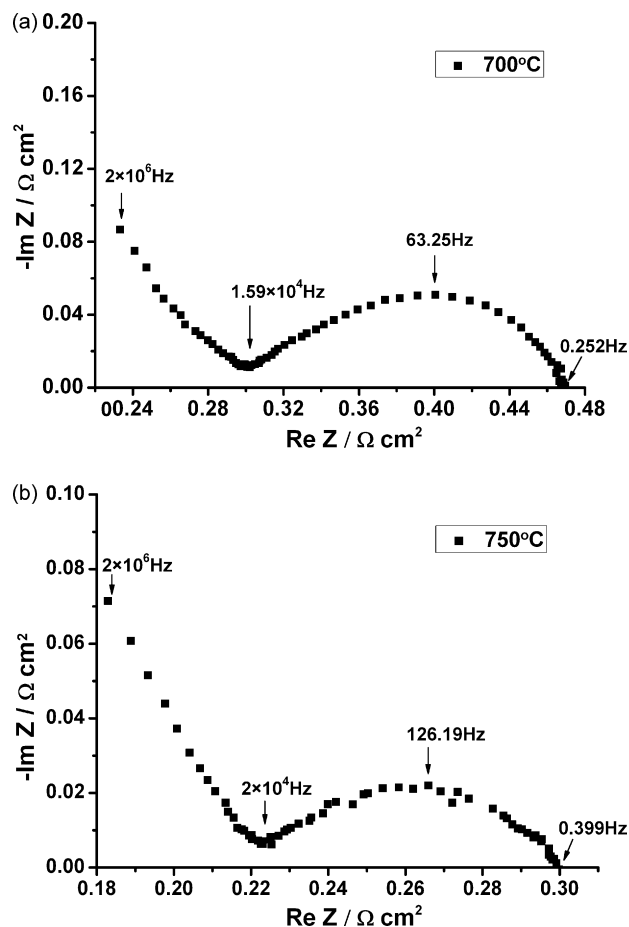


Fig. 8. Impedance spectra of the LSC/GDC/LSC symmetric cell obtained in air and OCV condition for different temperatures: (a) 700 °C and (b) 750 °C.

### 3.4. Bulk conductivity

The LSC powders synthesized from the precursor with Surfactant2 and a pH value of 0.5 were pressed into a bar and sintered at 1200 °C or 1250 °C for 5 h. Fig. 6 shows the electrical conductivity at various temperatures which was measured using four probe method. The sample sintered at 1250 °C exhibited high electrical conductivities of 2204 S cm<sup>-1</sup> at 600 °C and 1867 S cm<sup>-1</sup> at 800 °C.

### 3.5. Symmetric cell measurement

Fig. 7 displays the fracture morphology of the specimen of an LSC layer on a GDC substrate prepared via spray deposition. SEM photographs of the specimen indicated that sintering took place between the particles to form sintering necks, where a homogeneous and porous microstructure was formed, and the LSC thin film was well-knitted with the substrate. The electrochemical properties of the symmetrical cell of the porous LSC cathode were studied and the corresponding impedance spectra are given in Fig. 8. The  $R_p$  of the LSC cathode at 700 °C in air was only 0.17 Ω cm<sup>2</sup>; at 750 °C a low  $R_p$  of 0.07 Ω cm<sup>2</sup> was obtained, which demonstrated excellent activities at intermediate temperatures.

The utilization of this high performance cathode in cells based on a conventional YSZ electrolyte is highly preferred for practical applications; therefore, the cell configuration of LSC/GDC/YSZ using GDC as a barrier layer should be investigated in further studies.

## 4. Conclusions

The present work described the synthesis details of nanocrystalline La<sub>0.6</sub>Sr<sub>0.4</sub>CoO<sub>3-δ</sub> by the CA-EDTA complexing method. It has been found that the precursor preparation conditions, such as the pH value of the starting solution and the amount of surfactant addition, have a significant effect on the morphology of the oxide powders. With a pH value of 0.5, the La<sub>0.6</sub>Sr<sub>0.4</sub>CoO<sub>3-δ</sub> powder was obtained with a single perovskite phase at 900 °C. The addition of a proper amount of surfactant was determined and a uniform powder of LSC was achieved with an average particle size of about 60 nm; the agglomerate was greatly abated. The sintered LSC sample exhibited a high electrical conductivity of 1867 S cm<sup>-1</sup> at 800 °C. The porous cathode of LSC on the GDC electrolyte was prepared by spray deposition; the electrochemical measurement showed good performances at intermediate temperatures.

## Acknowledgments

This work was partly supported by the National High Technology Research and Development Program of China (863 Program, Grant No. 2007AA05Z140) and the Chinese Academy of Sciences.

## References

- [1] S.B. Adler, Chem. Rev. 104 (2004) 4791–4843.
- [2] R.M. Ormerod, Chem. Soc. Rev. 32 (2003) 17–28.
- [3] W.G. Wang, Y.-L. Liu, R. Barfod, S.B. Schougaard, P. Gordes, S. Ramousse, P.V. Hendriksen, M. Mogensen, Electrochem. Solid-State Lett. 8 (12) (2005) A619–A621.
- [4] W. Winkler, J. Koepfen, J. Power Sources 61 (1996) 201–204.
- [5] T. Kadowaki, T. Shiomitsu, E. Matsuda, H. Nakagawa, H. Tsuneizumi, T. Maruyama, Solid State Ionics 67 (1993) 65–69.
- [6] R.T. Leah, N.P. Brandon, P. Aguiar, J. Power Sources 145 (2005) 336–352.
- [7] J.W. Fergus, J. Power Sources 147 (2005) 46–57.
- [8] F.L. Lowrie, R.D. Rawlings, J. Eur. Ceram. Soc. 20 (2000) 751–760.
- [9] T. Tsai, S.A. Barnett, Solid State Ionics 93 (1997) 207–217.
- [10] S. Souza, S.J. Visco, L.C. De Jonghe, J. Electrochem. Soc. 144 (1997) L35–L37.
- [11] J.W. Kim, A.V. Virkar, K.-Z. Fung, K. Mehta, S.C. Singhal, J. Electrochem. Soc. 146 (1999) 69–78.
- [12] M. Mogensen, N.M. Sammes, G.A. Tompsett, Solid State Ionics 129 (2000) 63–94.
- [13] W.G. Wang, M. Mogensen, Solid State Ionics 176 (2005) 457–462.

- [14] V. Szabo, M. Bassir, A. Van Neste, S. Kaliaguine, *Appl. Catal. B: Environ.* 37 (2002) 175–180.
- [15] S. Nakayama, M. Okazaki, Y.L. Aung, M. Sakamoto, *Solid State Ionics* 158 (2003) 133–139.
- [16] V.V. Srdi'c, R.P. Omorjan, J. Seydel, *Mater. Sci. Eng. B* 116 (2005) 119–124.
- [17] N.P. Bansal, Z. Zhong, *J. Power Sources* 158 (2006) 148–153.
- [18] D. Berger, V. Fruth, I. Jitaru, J. Schoonman, *Mater. Lett.* 58 (2004) 2418–2422.
- [19] D. Berger, C. Matei, F. Papa, G. Voicu, V. Fruth, *Prog. Solid State Chem.* 35 (2007) 183–191.
- [20] M. Pechini, US Patent No. 3,330,697 (1967).
- [21] M. Popa, J. Frantti, M. Kakihana, *Solid State Ionics* 154 (155) (2002) 135–141.
- [22] Z. Shao, W. Yang, Y. Cong, H. Dong, J. Tong, G. Xiong, *J. Membr. Sci.* 172 (2000) 177–188.
- [23] W. Zhou, Z. Shao, W. Jin, *J. Alloys Compd.* 426 (2006) 368–374.
- [24] S. Lee, Y. Lim, E.A. Lee, H.J. Hwang, J.-W. Moon, *J. Power Sources* 157 (2006) 848–854.
- [25] Z. Bi, M. Cheng, Y. Dong, H. Wu, Y. She, B. Yi, *Solid State Ionics* 176 (2005) 655–661.
- [26] A.C. Pierre, *Introduction to Sol–Gel Processing*, 1st ed., Kluwer Academic Publishers, London, 1998, pp. 155–158.